Agarwal and Singh
Advances in Bridge Engineering (2023) 4:12
https://doi.org/10.1186/s43251-023-00090-5

Advances in
Bridge Engineering

ORIGINAL INNOVATION

Parametric study on prestressed skewed box-girder bridge

Preeti Agarwal[1] and Deepak Kumar Singh[2*]

*Correspondence:
erdeepak.India@gmail.com

[1] Department of Civil Engineering, Maharishi School of Engineering & Technology, MUIT, Lucknow, U.P. 226013, India
[2] Department of Civil Engineering, Amity School of Engineering & Technology, Amity University Patna, Bihar 801503, India

Abstract

This study employs the finite element-based CSiBridge v.20.0.0 software to examine the response of a single-cell prestressed box-girder bridge subjected to Indian loading conditions. The analyses is carried out on a simply supported bridge considering the specifications of Indian Road Congress (IRC) 6:2017, IRC 18:2000 and IRC 21:2000. An existing model of prestressed skewed bridge is validated with the published one. A convergence study is conducted for determining the model's mesh size. An extensive parametric study is carried out to gain a better understanding of the response of a skewed prestressed bridge. The parameters variables are: Skew angle (0°, 10°, 20°, 30°, 40°, 50°, and 60°); Span (35, 40, 45, 50, 55, and 60 m); and Span-depth ratio (10, 12, 14, 16 and 18). The results of this study are presented as ratios of Bending moment, Shear force, Torsional moment, and Vertical deflection. Finally, equations for estimation of these ratios for different span and span-depth ratio are also deduced from the statistical approach so that the results of skewed bridges may be evaluated directly. It is determined that the skewed bridge outperforms the straight bridge because of its higher span-depth ratio, which results in less bending moment development. Evidence suggests that the skewness may help to lessen the prestress load's dominance. The findings of this study may be helpful to engineers and designers in the analysis and design of prestresssed skewed box-girder bridges.

Keywords: Prestressed bridge, CSiBridge, Finite element method, Single-cell, Indian loading, Span, Skew angle, Span-depth ratio

1 Introduction

Construction requirements for transport systems have significantly improved as a result of the country's ongoing economic and infrastructure investment growths. The availability of land is diminishing in both industrialised and emerging nations. These days, box-girder bridges are being built because of their affordability, attractiveness, torsional rigidity, and other factors.

Most bridges are categorised as straight bridges and are supported orthogonally to the flow of traffic. But due to existing facilities and constraints, skewness is introduced during the construction of bridges. The skewness of the bridge is defined as the inclination of the abutments to the traffic normal as shown in Fig. 1a by Michigan skewed bridge. A skew box-girder bridge has girders that can be angled with the abutment at any

a) Michigan skewed bridge (Located at US)

Source:https://www.semanticscholar.org/paper/Skewed-Highway-Bridges-Fu-Chun/d70a4895bc41c52cb7a2c0fec8f67b43a7534ebb

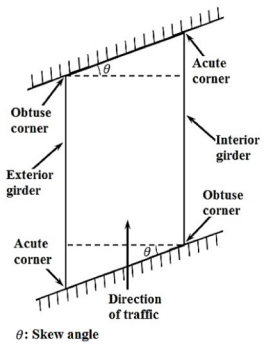

b) Mathematical model of skewed bridge

Fig. 1 Skewed Box-Girder Bridge Deck

angle other than 90 degrees as shown in Fig. 1b. As a result, skewed prestress box-girder bridges have quickly emerged as a viable alternative to handle traffic loads and more effectively utilise urban areas, since they have a great combination of bending, shearing, and torsion. Skewed bridges have a more complicated load transfer mechanism than straight bridges. The load distribution path in a straight bridge runs straight along the span direction. However, in a skewed bridge, the bridge load typically follows the obtuse corners of the bridge in a short path. This type of load transfer mechanism reduces longitudinal moment but increases transverse moment, shear force, and reaction at obtuse corner, while uplift and low reaction are possible at acute corner.

Using a semi-analytic approach, Brown and Ghali (1975) examined skew box girder bridges. It is assumed that the bridge is made up of parallelogrammatic strips. Experimental test results and numerical finite element results are used to validate the results of this method. Bakht (1988) reviewed the skewed bridges which are analysed as right bridges having skew angle less than 20°. Using this technique, longitudinal moments in skew slab-on-girder bridges are obtained with good accuracy. The error found by analysing the bridge as right bridge is characterised by dimensionless parameters. The skew angle, the spacing and span, and the girder's relative flexural rigidities influence these variables to the slab's flexural rigidity. The author for the analysis of skewed bridges also provides some recommendations. Chang (1992) investigated the effect of prestessed tendons on shear-lag of continuous box-girder bridges. Bishara et al. (1993) presented the distribution factor expressions for the interior and exterior girders of concrete composite bridges subjected to wheel load. The numerical results obtained are validated with the experimental results obtained from the tests performed on the actual models. The effect of girder spacing, skew angle, span, position of live load (AASHTO (American Association of State Highway Transportation Officials) loadings), etc. are also considered in the analysis. Ebeido and Kennedy (1995) looked into how skewness affected the shear distribution factor when OHBDC (Ontario Highway Bridge Design Code) truck loadings are applied. The effect of other factors like girder spacing, aspect ratio of bridge, no. of lanes, diaphragms are also considered in the study. The expressions for the shear distribution factors are derived from the results that are obtained. Helba and

Kennedy (1995) conducted a yield-line analysis on composite bridges model loaded by OHBDC truck loadings. The obtained results are compared with a nonlinear finite element analysis results. The results of the ultimate load up to failure of deck slabs are also presented. Ebeido and Kennedy (1996) performed finite element analysis on continuous (three span) and simply supported composite bridges. A parametric study is performed on different models by varying girder spacing, skewness, aspect ratio of bridge, span, etc. The obtained results are used to derive moment distribution factor expressions for both live and dead loads. The AASHTO and OHBDC truck loadings for continuous and simply supported bridges are considered, respectively. Ebeido and Kennedy (1996) investigated the effect of skewness and different design parameters on the shear and reaction distribution factors of continuous (two span) composite steel-concrete bridges using finite element method (FEM). The obtained results are validated with experimental results and used to deduce the expressions for shear and reaction distribution factors. Barr et al. (2001) evaluated flexural live-load distribution factors for a prestressed concrete girder bridges (three span) using finite element method. The results are evaluated considering the effect of lifts, diaphragms (intermediate and end), skewness, etc. Mo et al. (2003) experimentally investigated prestressed concrete box-girder bridges having corrugated steel webs. Further, analytical models have been prepared to predict the load-displacement relation of these type of bridges. Khaloo and Mirzabozorg (2003) investigated simply supported I-section concrete girder bridges using FEM. Varying girder spacing, span, skew angle, and different diaphragms arrangement determine the load distribution factors. Huang et al. (2004) studied the transverse load distribution on a skewed slab-on-steel girder bridges, both experimentally and numerically. The analysis comprised of a two span continuous bridge with 60° skew angle. The obtained results are compared with AASHTO formulas. Huang and Liu (2006) used FEM to analyse the response of a prestressed bridge having unbonded tendons under combined torsion, bending, and shear. The theoretical results are contrasted with a modified skew bending model. Conner and Huo (2006) looked into how parapets and a bridge's aspect ratio affected the moment distribution factor for a live load. Using FEM, the study is conducted on 34 continuous (two-span) bridges with skew angles of 0° or 45°. The results obtained are contrasted with those from the AASHTO method. Hughs and Idriss (2006) evaluated the shear and moment live-load distribution factors for an AASHTO truck-loaded prestressed concrete box-girder bridge. The factors are measured using fiber optic sensors and validated with a finite element model. Huo and Zhang (2006) used FEM to examine how different skew angles affected the live load reactions and shears of continuously skewed steel I-beam bridges. The distribution factors of reactions and shears are also compared. Menassa et al. (2007) used FEM to demonstrate the impact of skewness on simple-span reinforced concrete bridges while varying the span length, slab width, and skew angle under AASHTO truck loading. The analysis is performed on 96 different modelled bridges and the results are compared with reference straight bridge and AASHTO standard specifications. Huo and Zhang (2008) used finite element analysis to investigate the impact of skewness, which ranged from 0 to 60 degrees, on reactions at the piers and shear at beam ends of continuous bridges subjected to live loads. The analysis is performed on steel I-girder and prestressed concrete I-beam bridges. Huang et al. (2011) assessed the dynamic response of prestressed concrete bridges that

are subjected to moving vehicles. He et al. (2012) presented static and dynamic testing results for continuous, prestressed concrete box girder bridge models (1:8 scale) with 45° skew. Experiments are carried out to evaluate displacements and stresses, natural frequencies, mode shapes, and damping ratios, which are then compared to finite element results. Naser and Zonglin (2013) presented the structural performance of the skewed prestressed concrete bridges subjected to static and dynamic loads after repairing and strengthening of damaged members of bridge. The bridges are repaired and strengthened by treatment of cracks, thickening of web, adding internal pre-stressing tendons, introduction of cross beams between box girders. Mohseni and Rashid (2013) used SAP2000 finite element software to analyse skewed multicell box-girder bridges to determine stress distribution factors and deflection distribution factors. The analysis takes into account the effect of various parameters such as span, skew angle, number of lanes, and so on. Park et al. (2016) investigated the compatibility of concrete compressive strength and strand tensile strength, as well as the flexural behaviour of post-tensioned prestressed concrete girders reinforced with high-strength strands. Gupta and Kumar (2017) investigated the static and dynamic structural behaviour of skewed box girder bridges. The effect of skew angle on load distribution of single and multi-cell box girder bridges is also discussed. Further, Gupta and Kumar (2018) investigated the flexural response of skew-curved concrete box-girder bridge. Xue et al. (2018) analysed skewed box-girder using finite segment method, i.e., by converting three dimensional finite element method to one-dimensional model, thereby saving computations. A model test is also used to validate the proposed method. Zhu et al. (2019) experimentally investigated the structural response and failure mechanism of scaled (1:8) double deck prestressed concrete box-girder. Agarwal et al. (2019, 2020a,b, 2021) studied the reinforced concrete skewed and skew-curved box-girder bridges under Indian loading conditions using FEM. Authors also deduced some equations based on the study. Agarwal et al. (2022ab) presented the modelling and analysis procedures for box-grider bridges. The Indian Codal provisions are followed up to span of 50 m. Agarwal et al. (2022ab) evaluated the free vibration frequencies of box-girder bridges using FEM.

Based on the aforementioned literature review, the popularity of the box-girder bridges in different part of the world can be ascertained. The cited literature contains a significant quantity of research on I-girder and prestressed bridges, but no information is provided regarding the effects of dead load (DL), live load (LL), and prestress load (PL) on skewed bridges. Also, it seems that there hasn't been much research done on Indian standard loading. The literature on the combined effect of skew angle, span, and span-depth ratio in box-girder bridges is limited. In compared to a straight bridge, the study of skewed bridges is highly complicated. Due to their skewness, these are susceptible to a combination of bending and torsional moments. Under these circumstances, analytical procedures are ineffective and produce conservative results. Hence, finite element method is currently gaining popularity for such types of bridges because it delivers accurate findings faster and allows for the modelling of skewed bridges with varying degrees of complexity. In the present study, analysis of skewed prestress single cell trapezoidal box-girder bridge has been carried out by using finite based software CSiBridge v.20.0.0 under Indian loading conditions. Also, the effect of skew angle, span length and span-depth ratio on skewed box-girder bridge are investigated subjected to dead, live and

prestress loads. The effect of these parameters on forces and deflection for both girders has been investigated under Indian condition. For both girders, statistical approach has been used for determining the several equation to estimate the bending moment ratio (BMR), shear force ratio (SFR), torsional moment ratio (TMR), and vertical deflection ratio (VDR) under dead, live and prestress loads. The suggested equations will be helpful for the design of skewed box-girder bridges because they make it simple for designers to predict how skewed bridges would respond to dead, live and prestress loads using the data from a straight bridge. To validate this approach, results are verified with the results obtained by Hodson et al. (2012). After the analysis by reproducing the existing model of the literature, it has been observed that results obtained by the present approach shows a good agreement, as shown in Fig. 2. So, the modelling and analysis procedures are acceptable and extended to the parametric study on prestressed skewed box-girder bridge. Hence, the aim of the present investigation is to analyse a prestressed skewed box-girder bridge using CSiBridge.

2 Methodology

The parameters considered herein influence the design forces and deflection and also the analysis of skew bridges is complicated and time consuming; hence, these were selected for the parametric study so that the designers can directly deduce the values for selection of geometrical properties and preliminary analysis for their bridge models. Thus, the geometrical parameters, which directly affect the design of the bridge, are chosen for the parametric study, i.e., skew angle, span, and span-depth ratio. The purpose of this research is to look into how these parameters affect the forces and deflection of prestressed skewed box-girder bridges. The parameters are as follows: Skew angle = 0 to 60° at 10° intervals; span = 35, 40, 45, 50, 55, and 60 m; span-depth ratios = 10, 12, 14, 16, and 18 while keeping the span constant.

Parametric studies can be carried out experimentally, but it becomes quite complex to analyse bridges experimentally, also it consumes a lot of time to prepare a prototype. The software provide precise results in less time and have become popular nowadays to analyse complex structures like bridges. The modelling and analysis of prestressed trapezoidal 3- lane box-girder bridge is carried out by finite element based CSiBridge v.20.0.0 software. The behaviour of a prestressed box-girder bridge is investigated in this study by varying the skew angles, span, and span-depth ratio. Any structure can be modelled in two or three dimensions, but to assess the effect of loads on the entire bridge

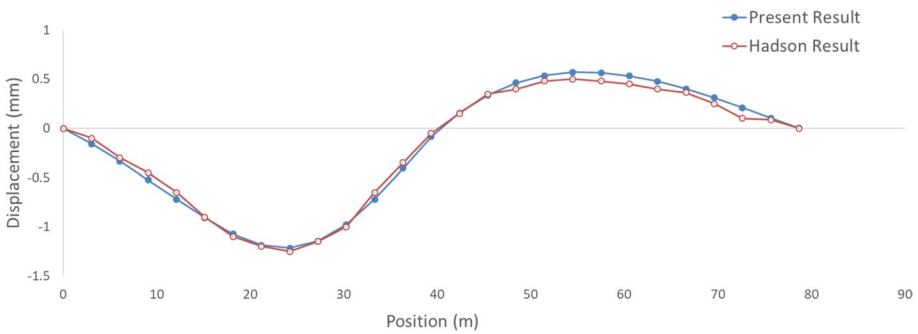

Fig. 2 Displacement comparison between test and present result

structure, the modelling must be done in three dimensions. The modelling and analysis in this study are carried out using the finite element-based software CSiBridge v.20.0.0, as shown in Fig. 3. The effects of kerb, footpath loads (wind, seismic, snow, creep, thermal, and fatigue) are neglected.

The deck data of prestressed bridge are: Total width = 12.25 m consisting of roadway width = 11.25 m with kerb = 0.5 m. Thickness of top slab, bottom slab and webs = 0.50 m. Figure 4 shows the cross-section of bridge model at support and mid span with the parabolic cable arrangement.

The bridge is modelled using the above cross-sectional properties and results (stresses and deflection) are evaluated for combined dead, live (3-lane IRC Class A) and prestress load. The results are within the limits specified in IRC:21-2000 and IRC:112-2011, the model is finalised.

M40 grade of concrete is used for the modelling of bridge. The material properties of prestressing cables are: Type of cable used = 19T15, Nominal area of cable = 26.6 cm^2, UTS of cable: 1860 MPa, Modulus of elasticity of cable: 2×10^5 MPa, Duct diameter: 150 mm, Wobble coefficient: 0.002, Friction coefficient: 0.17, Slip: 6 mm.

The bridge is modelled using a simply supported boundary condition, and discretised into four noded shell elements with six degrees of freedom at each node as shown in Fig. 5. Results converge after a mesh size of 100 mm, so it is used for discretisation. The primary loads considered in this study are dead load (self-weight of the bridge deck),

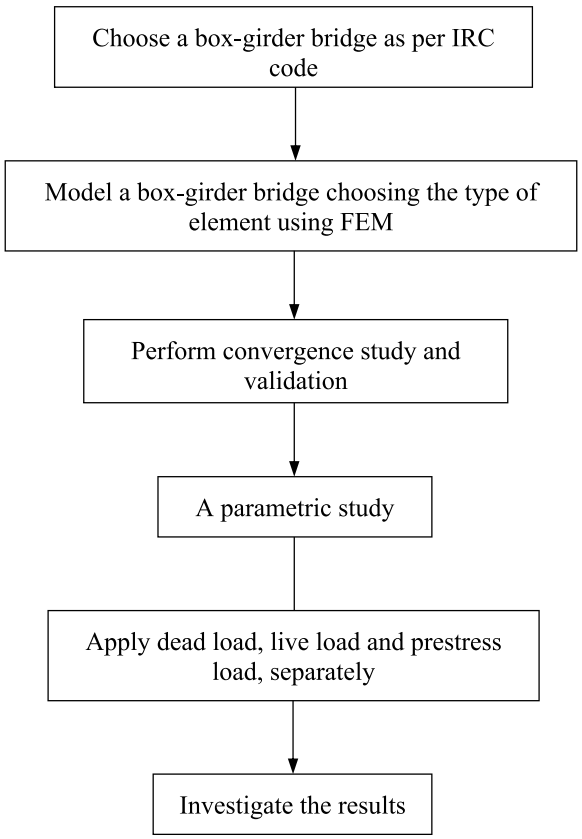

Fig. 3 Flow diagram of the parametric study

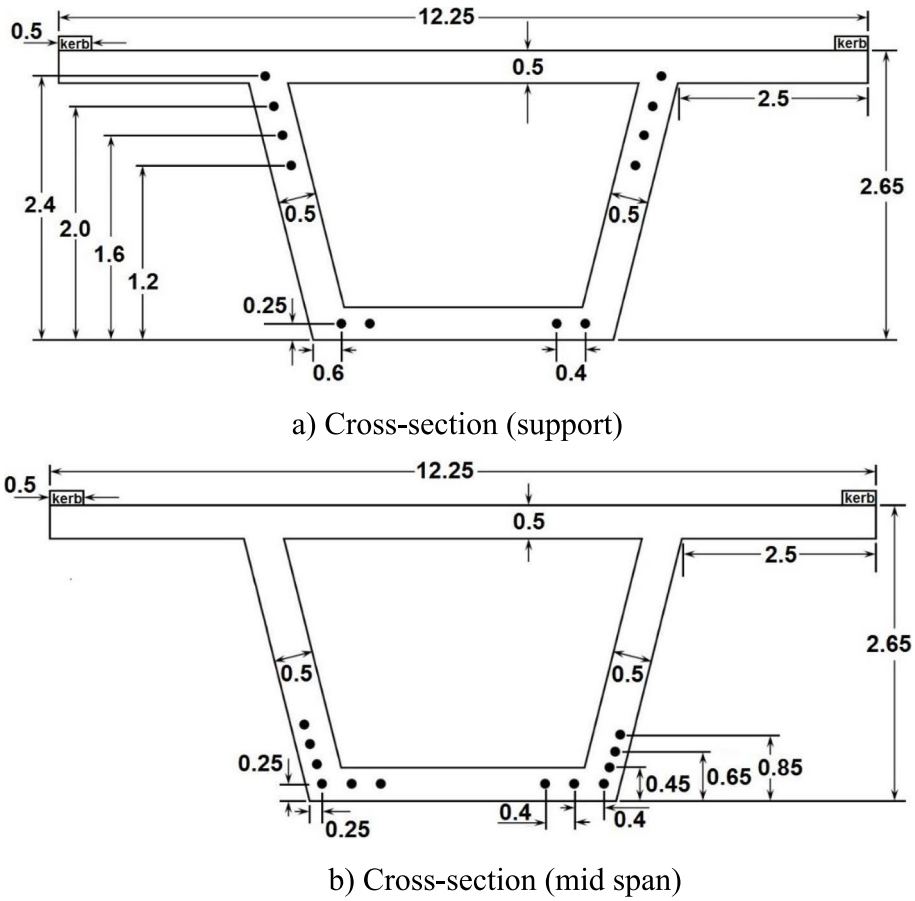

Fig. 4 Cross-section of the bridge (all dimension in metres)

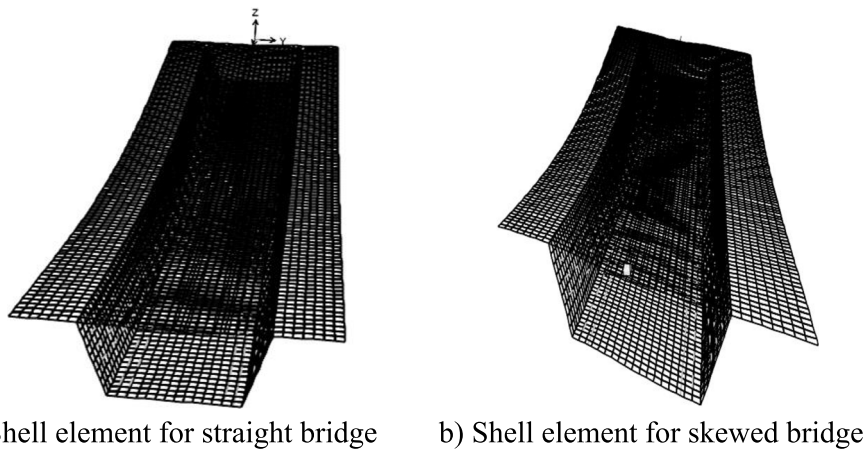

Fig. 5 Finite element model of bridge

live load (IRC:6-2017), and prestress load. IRC:6-2017 specifies the combination of different live loads for bridge analysis. One lane of Class 70 R for every two lanes, with one lane of Class A on the remaining lane, or three lanes of Class A for a three-lane highway.

Because the obtained forces and deflection are maximum for 3-lane IRC class-A load, it is considered and applied at a distance of 0.15 m from the edge of the kerb in this study.

3 Result and discussion

Maximum values in the form of ratios of the bending moment (BM), shear force (SF), torsional moment (TM), and vertical deflection (VD) are determined in the study in a single-cell prestressed trapezoidal box-girder bridge, separately under dead, live, and prestress loads and denoted as bending moment ratio (BMR_L), shear force ratio (SFR_L), torsional moment ratio (TMR_L), and vertical deflection ratio (VDR_L). BMR_L is defined as the maximum bending moment for any span of a skewed bridge under either DL, LL, or PL divided by the maximum bending moment for a 35 m span length of a straight bridge for the corresponding loadings. The definitions and implementation of all the other ratios are the same. The effect of various parameters such as span, span-depth ratio, and skew angle on bridge response is investigated. Furthermore, several equations are proposed for predicting forces and vertical deflection in prestressed skewed box-girders using a statistical approach based on least square regression. For validation, the proposed equations' results are compared to the analytical results. The effects of various parameters on the response of prestressed skewed box-girder bridges are discussed in the following sections.

3.1 Effect of skew angle and span

The influence of the skew angle and span on the forces and deflection is investigated herein. Figure 6 illustrates the relationship between BMR_L and bridge span for various skew angles under DL, LL, and PL. The skew angle's effect on the bending moment ratio under DL ($BMR_{L,DL}$) of both girders is observed to be non-linear and not particularly significant, whereas the effect of span length increases significantly with span. Both girders experience the same effects of skew angle and span on $BMR_{L,\,DL}$. According to the location of the section, it decreases as the skew angle increases. The span length has a significant impact on the bending moment ratio under live load ($BMR_{L,LL}$), and it exhibits nearly linear variation, but the effect is more on $BMR_{L,\,DL}$. In the case of the outer girder, the impact of the skew angle and the span on the $BMR_{L,LL}$ is greater, whereas the impact in the inner girder is negligible. Because the prestressing load is the same throughout the entire bridge span, the bending moment ratio under prestress load ($BMR_{L,PL}$) decreases with the span. In the case of an inner girder, skew angle and span length have a greater impact on $BMR_{L,PL}$. Up to a 20° skew angle, the outer girder's skew angle increases; after that, it decreases in both girders. On $BMR_{L,\,PL}$, skew angle has no appreciable impact.

When span length is varied from 35 m-60 m, the $BMR_{L,DL}$ in both the girders becomes about 2.9 times for the skew angle is increased from 0–60°. In outer girder, the $BMR_{L,LL}$ becomes about 2 times for the above variation while in case of inner girder it increases by about 1.9 times. When L/d is varied, the $BMR_{L,PL}$ in outer girder decreases by about 5.5% for the skew angle 0–60°; while in inner girder, it decreases by about 5.6–11.7% compared to the straight bridge having L/d of 10.

Figure 7 illustrates how SFR_L varies with span for various skew angles. The maximum shear force ratio under DL ($SFR_{L,DL}$) and the maximum shear force ratio under LL ($SFR_{L,LL}$) are observed to increase with span in both girders, with under DL experiencing

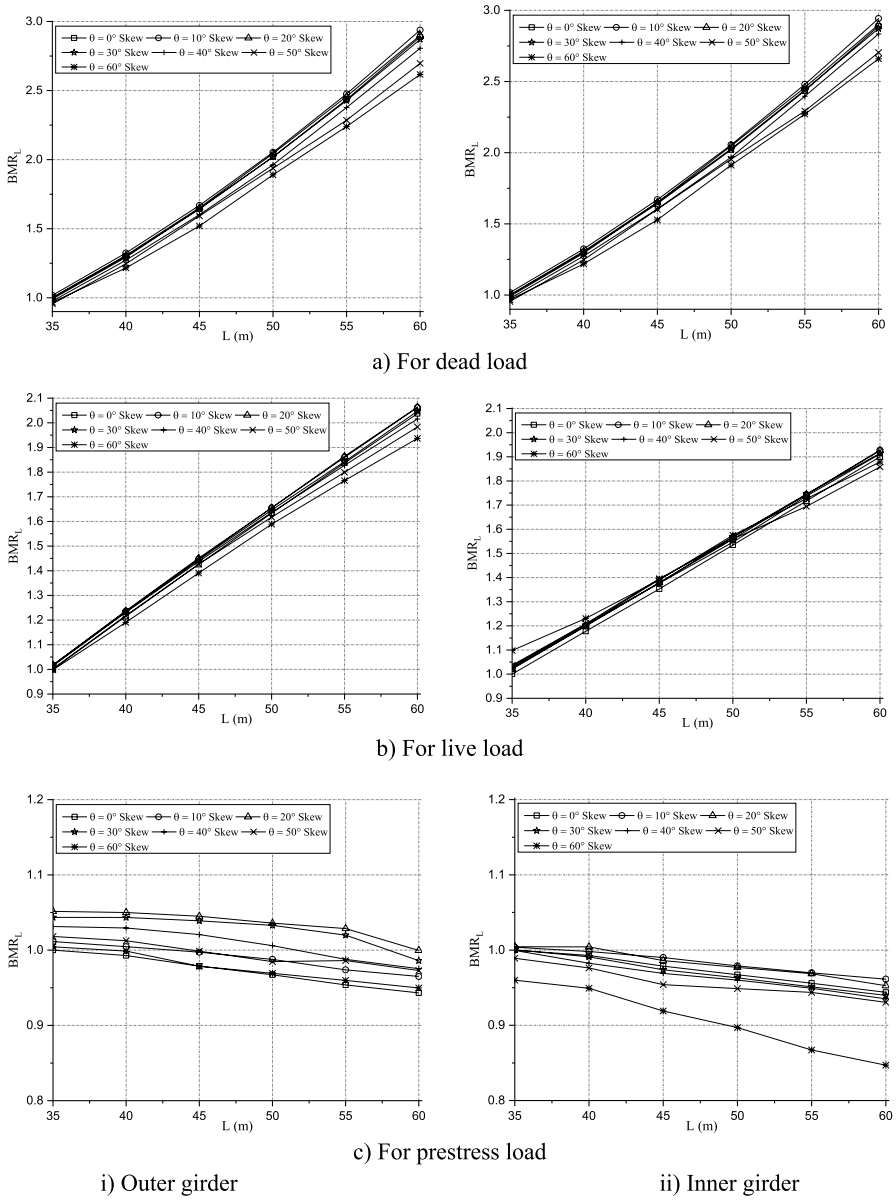

Fig. 6 Variation of bending moment ratio with span length for different skew angles

the largest increase. With increasing span, both girders' maximum shear force ratio under PL ($SFR_{L,PL}$) decreases. Because the prestressing load is the same throughout the entire bridge span, the shear force ratio under prestress load ($SFR_{L,PL}$) decreases with the span In both girders, the SFR increases with skew angle. In straight bridges, the girders are 90° perpendicular to the abutment; however, in skewed bridges, the girders make larger (obtuse) or smaller (acute) angles. Thus, the effect of loads (both dead and live) is more pronounced near the supports in skewed bridges than it is in straight bridges, which has the opposite effect. As a result, the SFR—a measure of the design shear forces in a skewed and a straight bridge—increases with the skew angle. In comparison to the inner girder, the span length and skew angle have a significantly greater impact on the

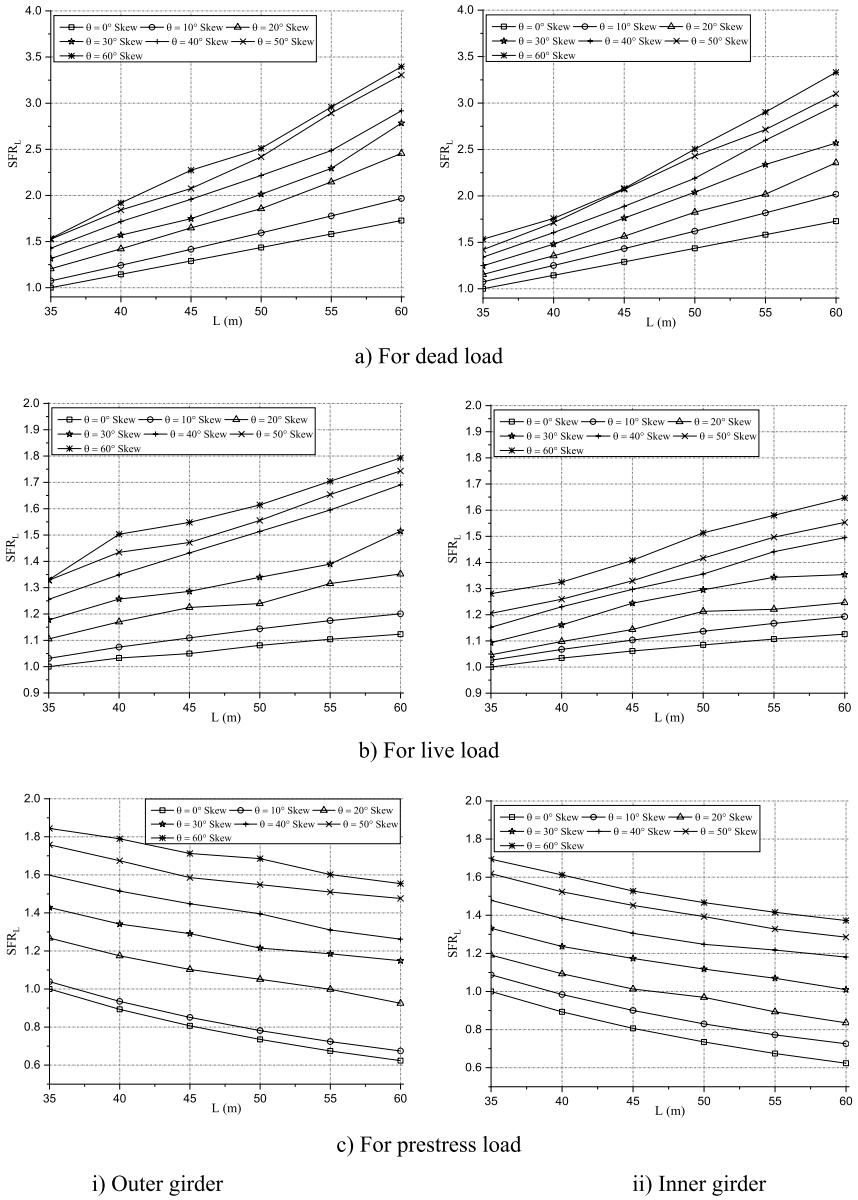

Fig. 7 Variation of shear force ratio with span length for different skew angles

outer girder. Compared to $SFR_{L,DL}$ and $SFR_{L,LL}$, $SFR_{L,PL}$ is significantly less affected by variation in span.

The increase in $SFR_{L,DL}$ of both girders for the skew angles variation from 0 to 60° is found to be approximately 1.7–2.2 times when the span length increases from 35 to 60 m. However, the $SFR_{L,LL}$ in both the girders is not influenced much by the variation in span length, irrespective of the skew angle. The increment in $SFR_{L,LL}$ of both the girders is found to be about 12–30% for the skew angles variation from 0 to 60°; while, the decrement in $SFR_{L,PL}$ is about 37–15% with the respective changes.

Figure 8 depicts the variation of the torsional moment ratio (TMR_L) in both girders with span length for different skew angles. The maximum torsional moment ratio under DL ($TMR_{L,DL}$) increases significantly and non-linearly with span length and skew angle

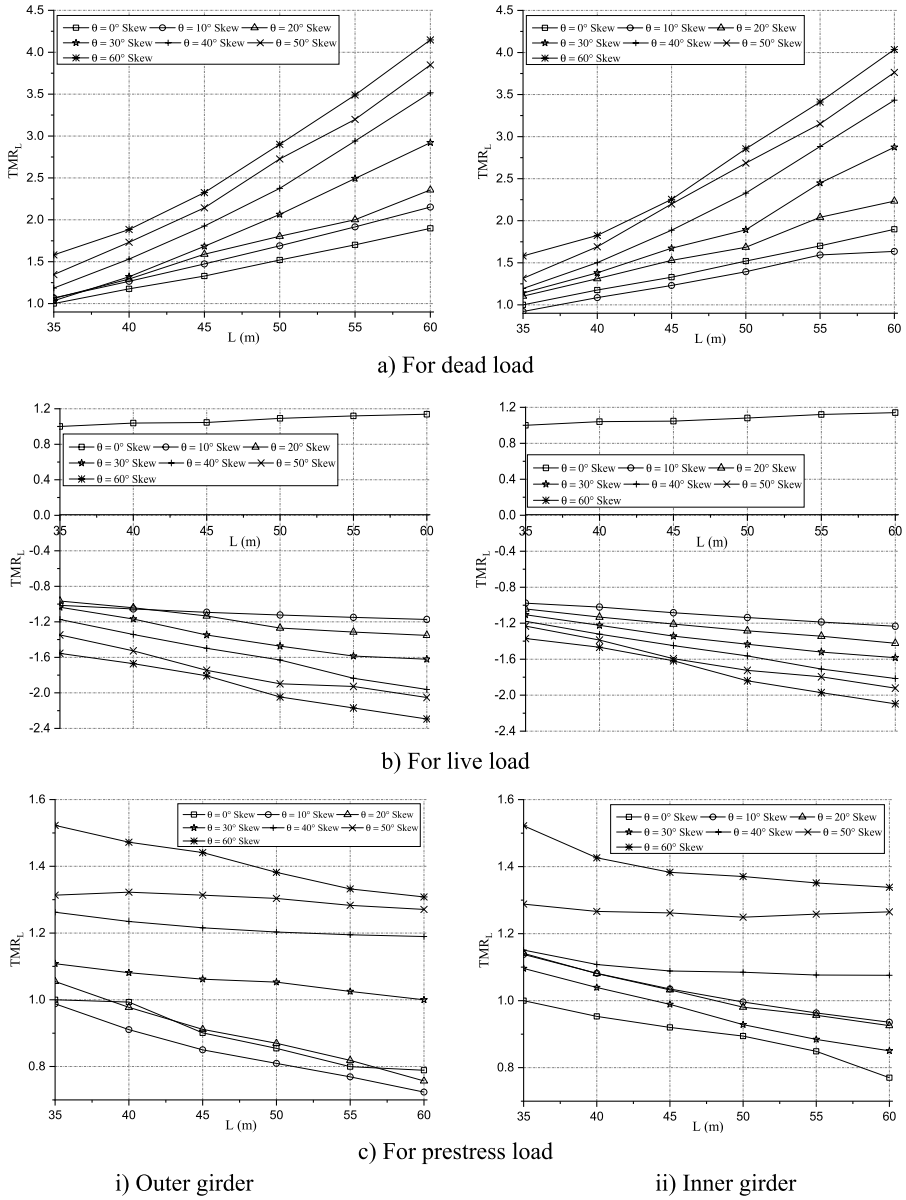

Fig. 8 Variation of torsional moment ratio with span length for different skew angles

in both girders, and the effect of skew angle increases significantly after a certain span length and depending on girder location. The $TMR_{L,DL}$ values are roughly same for both the girders. The effect of span on torsional moment ratio under LL ($TMR_{L,LL}$) is not significant in either girder; however, it increases with skew angle in both girders. A smaller skew angle (30°) has no effect on $TMR_{L,LL}$. Skew angle has a greater impact on the outer girder than the inner girder. The behaviour of $TMR_{L,LL}$ in the skewed bridge is opposite to that of the straight bridge, where it changes sign in both girders. In skew bridges, the value and the sign of the torsional moment is dependent on the load placement vis-à-vis the exterior and interior girder. Further, the placement of load along the span also influences the values. However, in case of straight bridges, the values of torsional moment in both the girders are same, except when the load placement is eccentric. The torsional

moment changes sign and thus the related TMR is plotted below the axis (on negative side).The behaviour of $TMR_{L,LL}$ in both girders is different in the skewed bridge than it is in the straight bridge, where it changes sign. The torsional moment ratio under PL ($TMR_{L,PL}$) is not significantly affected by span in either of the girders, but the skew angle effect is more due to PL.

The $TMR_{L,DL}$ in both girders is found to increase by about 2–2.6 times for a skew angle increase from 0 to 60° as the span length increases from 35 to 60 m. However, for different skew angles (13–47%), the $TMR_{L,LL}$ in both girders generally either increases slightly or stays almost constant. When the span length increases from 35 to 60 m, it is discovered that the $TMR_{L,PL}$ in both girders rises by about 23–12% for a corresponding increase in skew angle from 0 to 60°.

Figure 9 illustrates how VDR_L varies with span for various skew angles. The effect of skew angle increases slightly with span length while the vertical deflection ratio under DL ($VDR_{L,DL}$) increases significantly and non-linearly with both. As the skew angle increases, the $VDR_{L,DL}$ decreases. The vertical deflection ratio due to LL ($VDR_{L,LL}$) for both girders rises with span length and falls with skew angle increases. In contrast to outer girder, the effect of span length and skew angle on $VDR_{L,LL}$ is less pronounced in the case of inner girder. The span length has a significant impact on the vertical deflection ratio under PL ($VDR_{L,PL}$), which decreases significantly with skew angle. Due to the prestress load, the influence of span length and skew angle is reduced in VDR_L.

The $VDR_{L,DL}$ is found to increase by about 7–7.5 times for skew angles 0–60° when the span length for both girders is changed. The $VDR_{L,LL}$ increases by roughly 5.4–4.2 times in the outer girder for the aforementioned variation, while it rises by roughly 4.4–3.4 times in the inner girder. For the same variations in both girders, the $VDR_{L,PL}$ increases by roughly 2.5 times.

3.2 Effect of skew angle and span-depth ratio

The effects of span-depth ratio and skew angle are investigated for the bending moment ratio ($BMR_{L/d}$), shear force ratio ($SFR_{L/d}$), torsional moment ratio ($TMR_{L/d}$), and vertical deflection ratio ($VDR_{L/d}$). The box-girder bridges with span-depth ratio from 10 to 18 are considered in the study, as per the recommendation of IRC 21:2000. Here, the depth of girder is varied, keeping the span length constant, i.e., 35 m to obtain different span-depth ratios. The maximum bending moment in a straight bridge at a span-depth ratio of 10 for the appropriate loading is equal to the $BMR_{L/d}$, which is the ratio of the maximum bending moment at any span-depth ratio (L/d- 10, 12, 14, 16, and 18), to the maximum bending moment at span-depth ratio of 10 under either DL, LL, or PL. All the other ratios are defined and adopted similarly. The cross-sectional dimension of the deck is similar for different span-depth ratios.

Figure 10 shows the variation of $BMR_{L/d}$ in both the girders with the span-depth ratio for different skew angles. The graphs are plotted separately for DL, LL and PL. It is observed that for straight bridge the $BMR_{L/d}$ under DL ($BMR_{L/d,DL}$) decreases with L/d. This is because the depth is decreased with the increment in L/d. For both girders, the effects of span-depth ratio and skew angle on $BMR_{L/d,DL}$ are nearly identical. When L/d is varied, the $BMR_{L/d,DL}$ in both the girders decreases by about 39–36% for the skew angle 0–60° respectively, compared to the straight bridge having L/d of 10.

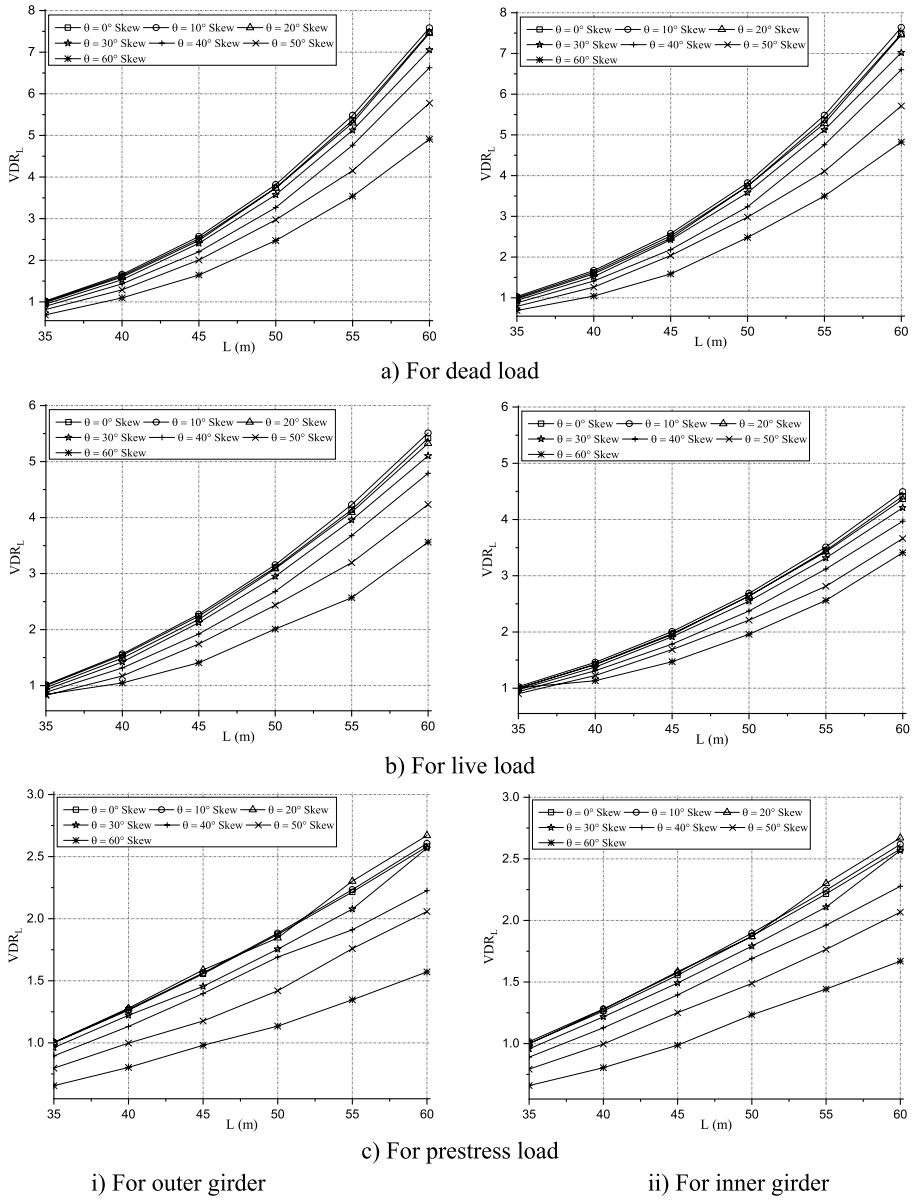

Fig. 9 Variation of vertical deflection ratio with span length for different skew angles

With an increase in L/d ratio, the $BMR_{L/d}$ under LL ($BMR_{L/d,LL}$) decreases significantly, and this effect is more pronounced in the case of the inner girder. In contrast, the effect of skew angle on the outer girder is negligible. The $BMR_{L/d,LL}$ in both the girders decreases with the increase in the L/d ratio; however, it increases with the skew angle. When L/d is increased from 10–18, and skew angle is increased from 0–60° the $BMR_{L/d,LL}$ increases by about 23–18%, compared to the straight bridge having L/d of 10, while in case of inner girder it decreases by about 26–22%.

With L/d, the $BMR_{L/d}$ under PL ($BMR_{L/d,PL}$) significantly decreases. But as the skew angle increases, $BMR_{L/d,PL}$ declines (insignificantly), and the effects of the span-depth ratio and skew angle are nearly identical for the two girders. When L/d is varied, the $BMR_{L/d,PL}$ in both the girders decreases by about 73%-77% for the skew angle 0–60°.

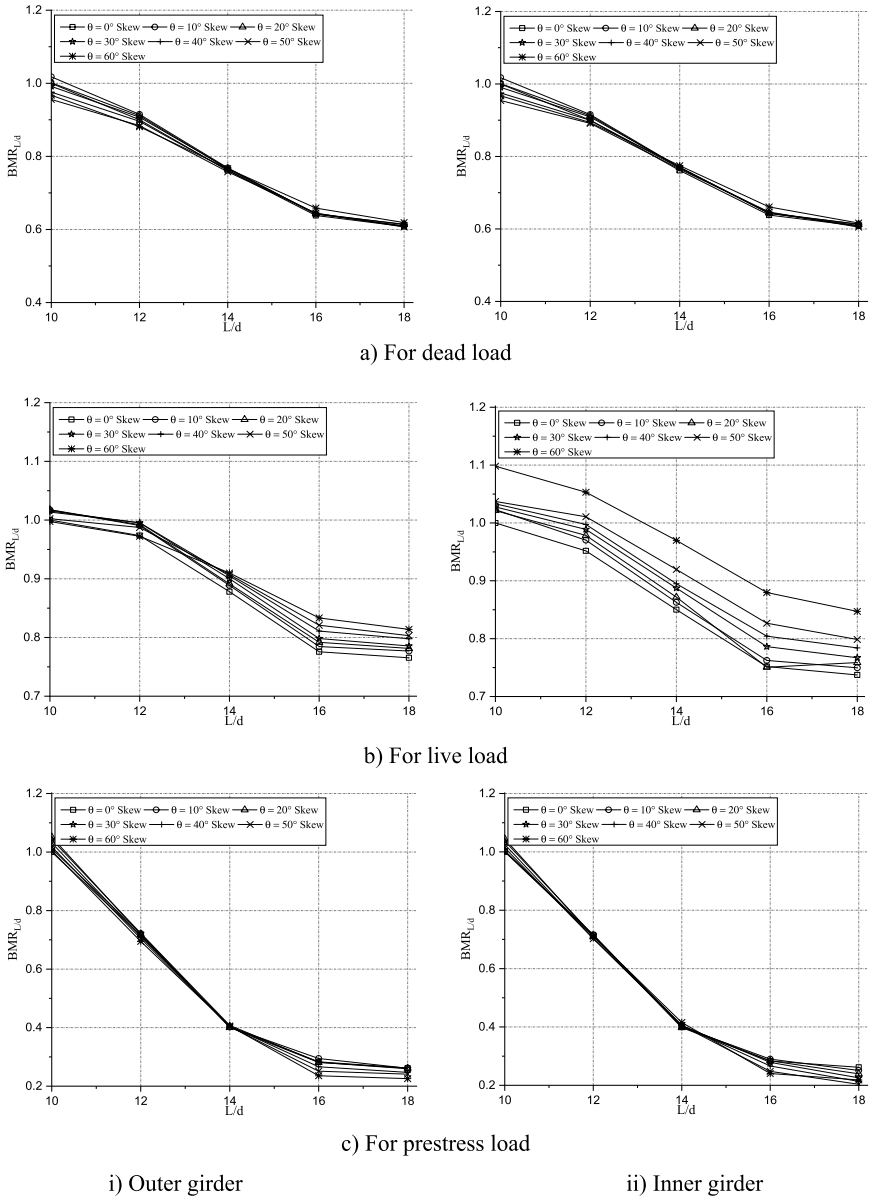

Fig. 10 Variation of bending moment ratio with span-depth ratio for different skew angles

Figure 11 shows the impact of L/d ratio on $SFR_{L/d}$ for various skew angles. In both girders, the $SFR_{L/d}$ increases with skew angle while decreasing with L/d ratio. The values of $SFR_{L/d,DL}$ is almost the same for both the girders. When the L/d is increased from 10–18, the increase in $SFR_{L/d,DL}$ is found to be about 15–10% for skew angle 0–60°, irrespective of the girder type.

For both the girders of a straight bridge, the $SFR_{L/d}$ under LL ($SFR_{L/d,LL}$) slightly increases with the L/d ratio. However, when a bridge skews, the effect is generally more pronounced in the outer girder and increases with both the span-depth ratio and skew angle. In comparison to a straight bridge, the $SFR_{L/d,LL}$ in the outer girder increases by roughly 4–7% for skew angles 10 to 60 degrees as the L/d is increased from 10 to 18, while the corresponding changes in the inner girder are only 1–4%.

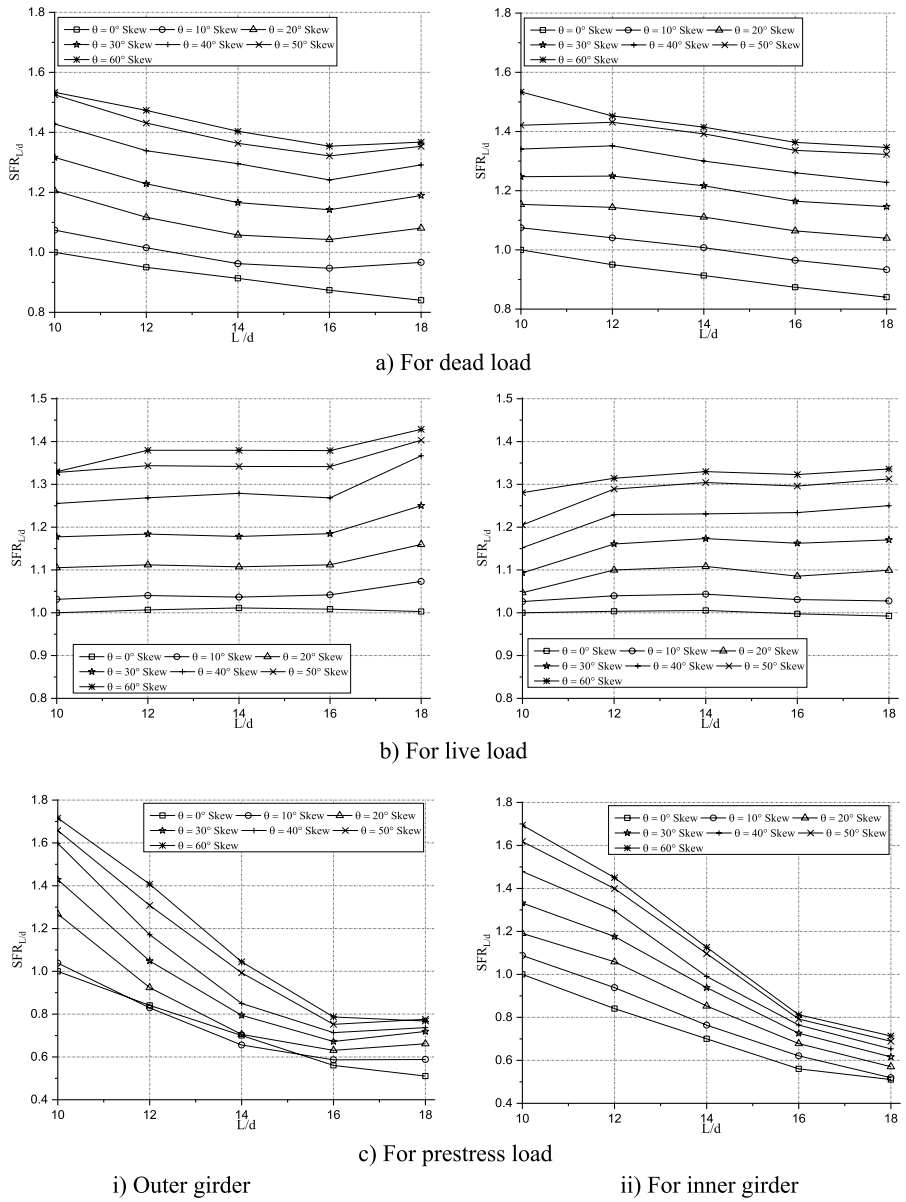

Fig. 11 Variation of shear force ratio with span-depth ratio for different skew angles

It is observed that for straight bridge the $SFR_{L/d}$ under PL ($SFR_{L/d,PL}$) decreases considerably with L/d up to 16. This is because the depth is decreased with the increment in L/d. For both girders, the effects of span-depth ratio and skew angle on $BMR_{L/d,DL}$ are nearly identical. When L/d is varied, the $SFR_{L/d,PL}$ in both the girders decreases by about 48–58% for the skew angle 0–60° respectively, compared to the straight bridge having L/d of 10.

The variation of $TMR_{L/d}$ in both girders, separately under DL, LL, and PL with L/d for various skew angles, is shown in Fig. 12. It has been found that the $TMR_{L/d}$ under DL ($TMR_{L/d,DL}$) increases with the skew angle while decreasing with the L/d ratio. The $TMR_{L/d,DL}$ in both girders decreases by about 35–10% for skew angles 0–60° when the L/d is increased from 10–18.

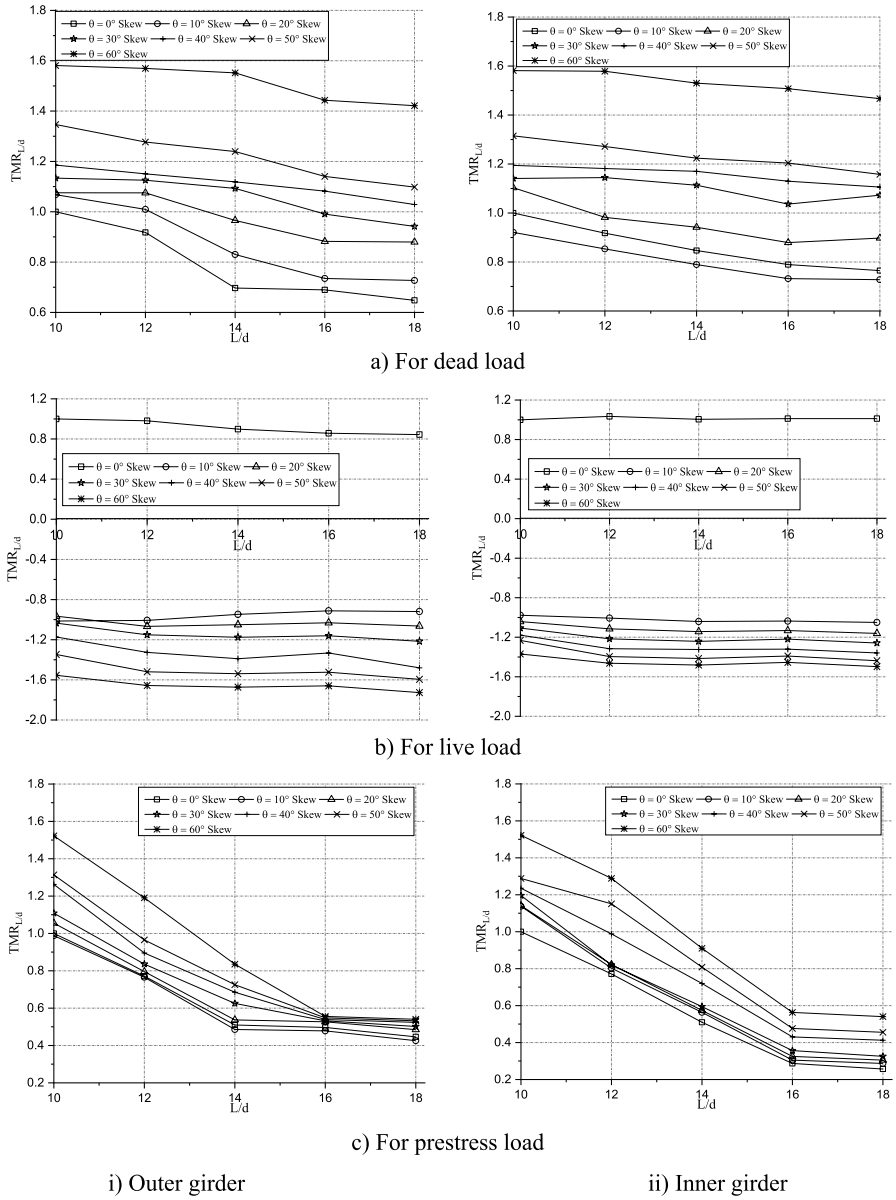

Fig. 12 Variation of torsional moment ratio with span-depth ratio for different skew angles

With the increase in L/d, the $TMR_{L/d}$ under LL ($TMR_{L/d,LL}$) in both girders slightly rises. The behaviour of $TMR_{L/d,LL}$ in both girders is different in the skewed bridge than it is in the straight bridge, where it changes sign. On $TMR_{L/d,LL}$, the impact of skew angles up to 30° is negligible, but for the outer girder, the impact is greater than for the inner girder. In outer girder, the $TMR_{L/d,LL}$ decreases by about 15% for bridge having skewness less than 30°; while for skewed bridges having skewness more than 30°, it increases by about 15–30% for outer girder and by about 9–15% for the inner girder.

The $TMR_{L/d}$ under PL ($TMR_{L/d,PL}$) in both the girders decreases significantly with span-depth ratio up to 16, after that the decrement is insignificant. But it increases with skew angle in both the girders. The impact of span-depth ratio and skew angle on $TMR_{L/d,PL}$ is the same for both girders. When the L/d is increased from 10–18, the

$TMR_{L/d,PL}$ in outer girders decreases by about 55–64% for skew angle 0–60°; while, for inner girder it decreases by about 74–64% for respective changes.

Figure 13 displays the $VDR_{L/d}$ with L/d variation for various skew angles. With L/d, the $VDR_{L/d}$ under DL ($VDR_{L/d,DL}$) increases. While the effects of span-depth ratio and skew angle are nearly identical for both girders, $VDR_{L/d,DL}$ decreases with an increase in skew angle. The least value is obtained at L/d ratio 10, and the deflection in skewed bridges is less than that in straight bridges. A skewed bridge is therefore better than a straight one. When L/d is varied, the $VDR_{L/d,DL}$ in both the girders increases by about 127% and 100% for the skew angle 0–60°, the increment being greater for the lesser angles.

The $VDR_{L/d}$ under LL ($VDR_{L/d,LL}$) increases with L/d in both girders. L/d has a greater impact on the straight bridge. In comparison to the inner girder, the outer girder is more

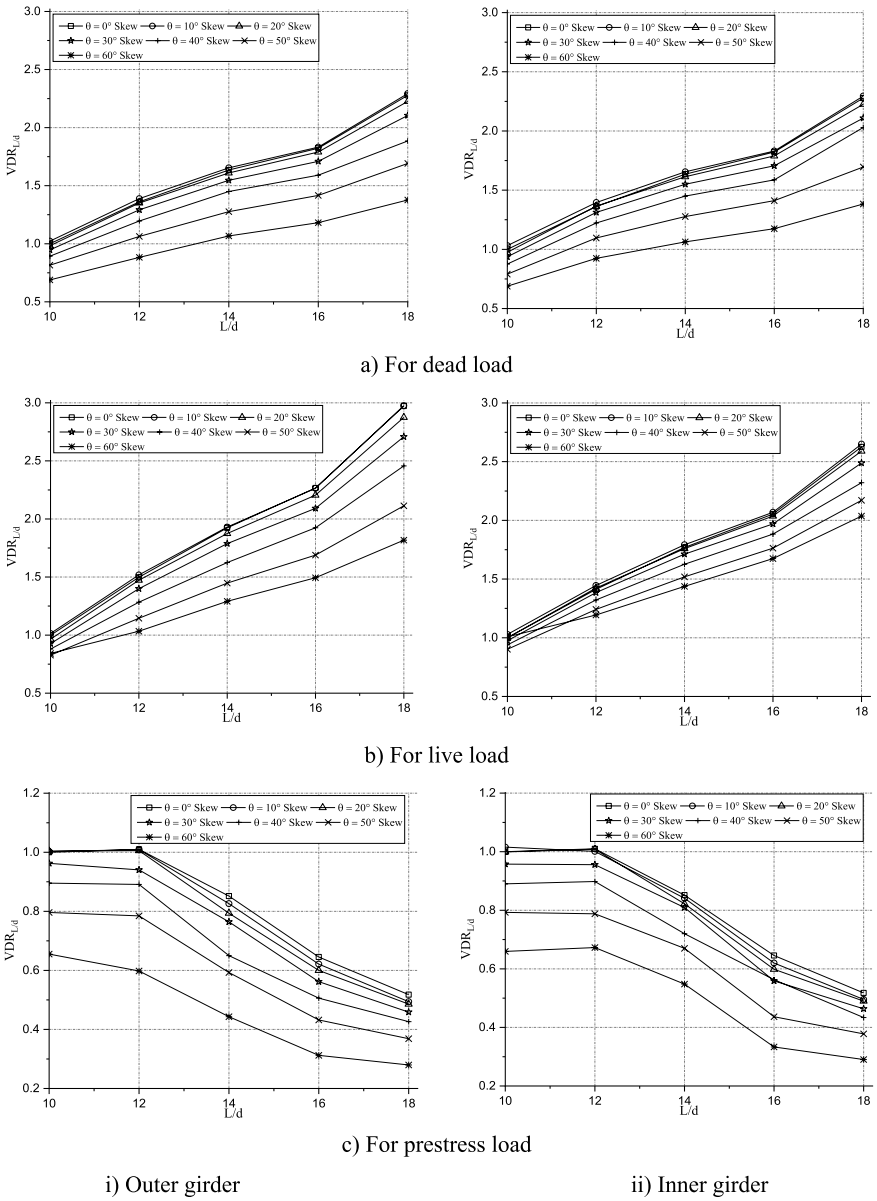

Fig. 13 Variation of vertical deflection ratio with span-depth ratio for different skew angles

affected by the L/d ratio and skew angle. As the skew angle increases, the effect gets smaller. When the L/d ratio is changed, the outer girder's $VDR_{L/d,LL}$ increases by about 195% and 115% for skew angles 0–60°, respectively, while the inner girder experiences increases of about 162% and 102%.

For both the girders, the $VDR_{L/d}$ under PL ($VDR_{L/d,PL}$) significantly decreases with the skew angle and L/d ratio greater than 12. This is due to reduction in spacing between tendons, when depth reduces. The effect is nearly same in both the girders. When the L/d is increased from 10–18, the $VDR_{L/d,PL}$ in both girders decreases by about 48–57% for skew angle 0–60°, compared to the straight bridge.

3.3 Relationship between responses and parameters

For a single cell trapezoidal skewed box-girder bridge, several equations are given to calculate the impact of skew angle, span, and span-depth ratio on different ratios for both the girders. For the purpose of obtaining the suggested equations, the three primary loads—dead load, IRC class – A load, and prestress load—are taken into separate consideration. With the help of the data gathered from the parametric study, a statistical method focused on least square regression is used for this objective. In order to calculate the combined effect of the skew angle and span when designing a skewed bridge, the designer may use the suggested equations. For DL, LL, and PL the following equations have been proposed:

3.3.1 Variation of span length and skew angle

For dead load

i) Outer girder

$$BMR = 0.1044 + 0.000776\,L^2 - 0.002038\,\theta \tag{1}$$

$$SFR = 0.0287\,L + 8.02384 \times 10^{-6}\theta L^2 \tag{2}$$

$$TMR = 0.03311\,L + 1.87479 \times 10^{-7}\theta L^3 - 0.20312 \tag{3}$$

$$VDR = 0.16607 + 5.8634 \times 10^{-7}L^4 - 6.0494 \times 10^{-11}L^4\theta^2 \tag{4}$$

ii) Inner girder

$$BMR = 0.065597 + 0.000788\,L^2 - 3.42599 \times 10^{-5}\theta^2 \tag{5}$$

$$SFR = 0.030239\,L + 7.9711 \times 10^{-6}\theta L^2 - 0.082208 - 5.61158 \times 10^{-7}\theta^3 \tag{6}$$

$$TMR = 0.029449\,L + 1.54864 \times 10^{-5}\theta L^2 - 0.099306\sqrt{\theta} \tag{7}$$

$$VDR = 3.63027 \times 10^{-5}L^3 - 0.55594 - 1.67626 \times 10^{-7}L^2\theta^2 \tag{8}$$

For live load

i) Outer girder

$$BMR = 0.040811\,L - 0.38871 - 1.51932 \times 10^{-5}\theta^2 \tag{9}$$

$$SFR = 0.79886 + 0.005421\,L + 1.931 \times 10^{-4}L\theta \tag{10}$$

$$TMR = 1.05716 + 0.28718\,\theta + 2.24008 \times 10^{-5}\theta^3 - 1.39213\sqrt{\theta} - 6.429 \times 10^{-4}L\theta - 0.0034467\theta^2 \tag{11}$$

$$VDR = 0.012684\,\theta + 2.51993 \times 10^{-5}L^3 - 0.1024843 - 1.0812911 \times 10^{-5}L\theta^2 \tag{12}$$

ii) Inner girder

$$BMR = 0.03528\,L + 3.2567 \times 10^{-4} - 0.216533 \tag{13}$$

$$SFR = 0.79211 + 0.00556064\,L + 1.74582 \times 10^{-4}L\theta - 0.0017525\,\theta \tag{14}$$

$$TMR = 1.04489 + 0.161507\,\theta - 1.063752\sqrt{\theta} - 5.5555 \times 10^{-4}L\theta - 7.416 \times 10^{-4}\theta^2 \tag{15}$$

$$VDR = 0.1654 + 0.004382\,\theta + 1.97398 \times 10^{-5}L^3 - 1.05291 \times 10^{-7}L^2\theta^2 \tag{16}$$

For prestress load

i) Outer girder

$$\begin{aligned} BMR = {} & 1.05348 + 2.0397 \times 10^{-4}\theta + 0.005724SIN(\theta) \\ & + 5.510922 \times 10^{-6}L\theta COS(\theta) - 2.16167 \times 10^{-5}\theta^2 \\ & - 0.0298244COS(0.1174748\theta) \end{aligned} \tag{17}$$

$$SFR = 1.37154 + 0.0424904theta - 0.012555\,L - 0.106834\sqrt{\theta} - 2.21792 \times 10^{-4}\theta^2 \tag{18}$$

$$\begin{aligned} TMR = {} & 1.42755 + 3.255707 \times 10^{-4}\theta^2 + 1.17727 \times 10^{-5}L\theta^2 \\ & - 0.0113079\,L - 0.01368487\,\theta - 1.805577 \times 10^{-7}L\theta^3 \end{aligned} \tag{19}$$

$$VDR = 0.18334 + 0.00631135\,\theta + 6.66537 \times 10^{-4}L^2 - 5.97245 \times 10^{-6}L\theta^2 \tag{20}$$

ii) Inner girder

$$\begin{aligned} BMR = {} & 1.084 + 1.09847 \times 10^{-6}\theta L^2 - 0.002335\,L - 6.470106 \times 10^{-8}\theta^3 \\ & - 2.680573 \times 10^{-10}L^2\theta^3 - 8.91315 \times 10^{-7}\theta L^2 COS(COS(\theta)) \end{aligned} \tag{21}$$

$$SFR = 0.1539 + 0.013008\theta + \frac{28.00977}{L} \tag{22}$$

$$TMR = 1.28309 + 0.00282\theta + 1.4978 \times 10^{-6} L\theta^2 - 0.007986L - 0.082041 * SIN(1.790689\theta - 9.83859 \times 10^{-4} L\theta) \quad (23)$$

$$VDR = 0.17057 + 0.0058052\,\theta + 6.7689 \times 10^{-4} L^2 - 5.5409 \times 10^{-6} L\theta^2 \quad (24)$$

3.3.2 Variation of span-depth ratio and skew angle

For dead load

i) Outer girder

$$BMR = 00.62276\left(\frac{L}{d}\right) + 0.0012823\left(\frac{L}{d}\right)^3 - 1.35673 - 1.454861 \times 10^{-4}\theta - 0.051596\left(\frac{L}{d}\right)^2 \quad (25)$$

$$SFR = 1.84 + 0.009429\,\theta + 0.00363859\left(\frac{L}{d}\right)^2 - 0.119303\left(\frac{L}{d}\right) \quad (26)$$

$$TMR = 1.50406 + 9.6901 \times 10^{-4}\left(\frac{L}{d}\right)\theta + 1.218534 \times 10^{-12}\left(\frac{L}{d}\right)\theta^6 - 0.0044377\theta - 0.05040515\left(\frac{L}{d}\right) - 2.3341619 \times 10^{-10}\left(\frac{L}{d}\right)^2\theta^4 \quad (27)$$

$$VDR = 0.151745\left(\frac{L}{d}\right) + 0.005364\theta - 0.496758 - 1.81561 \times 10^{-5}\left(\frac{L}{d}\right)\theta^2 \quad (28)$$

ii) Inner girder

$$BMR = 0.47918\left(\frac{L}{d}\right) + 2.67795 \times 10^{-5}\left(\frac{L}{d}\right)^4 - 1.06088 - 5.526136 \times 10^{-8}\theta - 0.0301427\left(\frac{L}{d}\right)^2 \quad (29)$$

$$SFR = 1.14708 + 0.0091659\,\theta - 0.016445\left(\frac{L}{d}\right) \quad (30)$$

$$TMR = 1.2481 + 2.56064 \times 10^{-4}\left(\frac{L}{d}\right)\theta + 0.00279849\,\theta + 6.21865 \times 10^{-7}\theta^4 - 0.027508\left(\frac{L}{d}\right) - 0.03040004\theta - 7.3399 \times 10^{-5}\theta^3 \quad (31)$$

$$VDR = 1.9852\left(\frac{L}{d}\right) + 0.0032582\left(\frac{L}{d}\right)^3 - 8.47611 - 0.135732\left(\frac{L}{d}\right)^2 - 1.174991 \times 10^{-5}\left(\frac{L}{d}\right)\theta^2 \quad (32)$$

For live load

i) Outer girder

$$BMR = 1.3425 + 5.447 \times 10^{-4}\theta + 0.03325\,COS\left(\frac{L}{d}\right) - 0.033071\left(\frac{L}{d}\right) \quad (33)$$

$$SFR = 1.00257 + 1.47543 \div 10^{-4}(\frac{L}{d})\theta + 2.230626 \times 10^{-4}\theta^2 - 2.54515 \times 10^{-6}\theta^3 \quad (34)$$

$$TMR = 0.217877\ \theta + 4.59293\ COS(-0.0316952\ \theta) - 3.646836 - 1.199406\sqrt{\theta} - 3.4319 \times 10^{-4}(\frac{L}{d})\theta \quad (35)$$

$$VDR = 0.23033(\frac{L}{d}) - 1.27601 - 9.32452 \times 10^{-7}(\frac{L}{d})^2\theta^2 \quad (36)$$

ii) Inner girder

$$BMR = 0.6722\left(\frac{L}{d}\right) + 0.0012792(\frac{L}{d})^3 + 2.7161 \times 10^{-5}\theta^2 - 1.7224 - 0.052774(\frac{L}{d})^2 \quad (37)$$

$$SFR = 0.98857 + 0.0017079\left(\frac{L}{d}\right)\theta - 0.00724\theta - 5.43725 \times 10^{-5}\theta(\frac{L}{d})^2 \quad (38)$$

$$TMR = 1.20455 + 0.13611\ \theta - 0.014071\left(\frac{L}{d}\right) - 1.03537\sqrt{\theta} - 7.3216 \times 10^{-4}\theta^2 \quad (39)$$

$$VDR = 0.19516(\frac{L}{d}) - 0.93033 - 5.06675 \times 10^{-7}(\frac{L}{d})^2\theta^2 \quad (40)$$

For prestress load

i) Outer girder

$$BMR = 0.050748(\frac{L}{d}) + \frac{27.7531}{\left(\frac{L}{d}\right)} + 0.0501023 * COS(0.894888 + \frac{L}{d}) - 2.245149 - 3.4427 \times 10^{-4}\theta \quad (41)$$

$$SFR = 3.27078 + 0.0268564\ \theta + 3.5568 \times 10^{-4}(\frac{L}{d})^3 - 0.262523\left(\frac{L}{d}\right) - 0.00135511(\frac{L}{d})\theta \quad (42)$$

$$TMR = 3.787059 + 0.01201588(\frac{L}{d})^2 + 3.1358 \times 10^{-4}\theta^2 - 0.399304(\frac{L}{d}) - 1.677347 \times 10^{-5}(\frac{L}{d})\theta^2 \quad (43)$$

$$VDR = 1.400145\left(\frac{L}{d}\right) + 0.00234589(\frac{L}{d})^3 + 1.33822 \times 10^{-9}(\frac{L}{d})^4\theta^2 - 5.00663 - 0.102974\left(\frac{L}{d}\right)^2 - 1.1199 \times 10^{-5}(\frac{L}{d})\theta^2 \quad (44)$$

ii) Inner girder

$$BMR = 0.0333524\left(\frac{L}{d}\right) + \frac{24.74359}{\left(\frac{L}{d}\right)} + 0.04698034\ COS(0.9994435 + \frac{L}{d}) - 1.794246 \quad (45)$$

$$SFR = 2.291731 + 0.022719\theta + 0.0036908\left(\frac{L}{d}\right)^2 - 0.166074\left(\frac{L}{d}\right) - 0.001062635\left(\frac{L}{d}\right)\theta \tag{46}$$

$$TMR = 4.28542 + 0.01172846\left(\frac{L}{d}\right)^2 + 1.04175 \div 10^{-4}\theta^2 + 0.0754635\, SIN\left\{-0.0284241\left(\frac{L}{d}\right)^2\right\} - 0.4354356\left(\frac{L}{d}\right) \tag{47}$$

$$VDR = 1.70608\left(\frac{L}{d}\right) + 0.00287256\left(\frac{L}{d}\right)^3 - 6.417106 - 8.612803 \times 10^{-5}\theta^2 - 0.125001\left(\frac{L}{d}\right)^2 \tag{48}$$

Some of the results of the BM, SF, and TM in single cell box girder bridges, separately under dead and live loads, obtained from the analysis are presented in Tables 1 and 2 along with the percentage error for span and span-depth ratio, respectively, for the validation of the aforementioned proposed equations. In every instance, it can be seen that the conclusions drawn from the equations closely match those of the finite element analysis. Therefore, it is simple to predict the forces and deflection in a skewed box-girder bridge using the proposed equations.

4 Conclusions

The finite element method (FEM) was used to analyse a prestressed skewed box-girder bridge under Indian loadings. The maximum values of the forces and deflection were calculated through comprehensive parametric studies. The parameters considered for investigation are skew angle, span length, and span-depth ratio. The ratios (forces and deflection) that represent the results of parametric studies on various trapezoidal box-girder bridges may be useful to designers in understanding behaviour and in providing appropriate guidelines for the cost-effective and logical design of these bridges.

The main conclusions drawn from the studies on prestressed skewed box-girder bridges can be summarised as follows:

- In comparison to live and prestress loads, the effect of skew angle on forces and deflection of both girders due to dead load is more significant.
- The forces and deflection increase nonlinearly with span for all the bridges.
- Up to 30°, the effect of skew angle on the forces and deflection ratios is negligible; therefore, such bridges can be analysed and treated as straight bridges.
- Under dead and live loads, the BMR_L rises with span in both girders; however, under prestress loads, it slightly falls. Additionally, skew angle has little impact on BMR_L. The skewed bridge is superior to the straight bridge because it develops less bending moment due to its higher span-depth ratio.
- The shear force in both girders increases significantly with the skewness for both the girders under all load conditions. The SFR increases with span under dead and live loads, and it decreases considerably under prestress load. The SFR decreases with span-depth ratio in all the load conditions.
- As the skew angle rises, the torsional moment in both girders rises as well. While the TMR_L under DL only slightly increases with span length, it does significantly

Table 1 Verification of various ratios with span for different skew angles

Forces	Girder	Span (m)	Skew angle (degree)	For dead load			For live load			For prestress load		
				Using proposed equation	Using FEM	% variation	Using proposed equation	Using FEM	% variation	Using proposed equation	Using FEM	% variation
BM (kNm)	Outer	40	30	23,666	23,817	0.632	5840	5857	0.297	-27,129	-26,625	-1.892
	Inner	35	30	18,420	18,247	-0.948	5288	5286	-0.031	-25,509	-25,527	0.071
SF (kN)	Outer	55	50	-6202	-6425	3.471	-852	-866	1.545	3362	3393	0.922
	Inner	35	40	2956	2978	0.730	872	865	-0.789	-3315	-3324	0.283
TM (kNm)	Outer	60	40	-6047	-6248	3.210	-1036	-1078	3.907	3163	3245	2.534
	Inner	55	20	-3754	-3626	-3.509	-950	-919	-3.400	2585	2609	0.944
VD (mm)	Outer	45	10	-21.89	-22.11	0.998	-4.29	-4.30	0.092	18.424	18.356	-0.369
	Inner	60	0	-62.65	-64.32	2.584	-10.98	-10.95	-0.314	30.608	30.289	-1.053

Table 2 Verification of various ratios with span-depth ratio for different skew angles

Forces	Girder	Span-depth ratio	Skew angle (degree)	For dead load			For live load			For prestress load		
				Using proposed equation	Using FEM	% variation	Using proposed equation	Using FEM	% variation	Using proposed equation	Using FEM	% variation
BM (kNm)	Outer	16	30	11,914	11,828	-0.721	3788	3790	0.042	-6948	-7186	3.304
	Inner	12	40	16,652	16,574	-0.471	5136	5130	-0.100	-18,132	-17,957	-0.976
SF (kN)	Outer	14	10	-2171	-2138	-1.541	-546	-543	-0.605	1462	1474	0.832
	Inner	18	20	2298	2309	0.493	831	826	-0.633	-1281	-1282	0.058
TM (kNm)	Outer	10	60	-2810	-2810	0	-860	-855	-0.503	4149	4153	0.117
	Inner	14	60	-2725	-2719	-0.240	-1013	-1013	0	2489	2483	-0.263
VD (mm)	Outer	10	40	-8.12	-7.68	-5.82	-1.66	-1.66	0	10.396	10.512	1.101
	Inner	12	30	-11.22	-11.29	0.623	-3.34	-3.43	2.799	11.058	11.219	1.434

increase under LL. However, it falls off as the span-depth ratio rises. The behaviour of TMR under LL in the skewed bridge is different from that of the straight bridge in both girders.

- The deflection is less in skewed bridges and increases with span-depth ratio under DL and LL, and the minimum value is obtained at a span-depth ratio of 10. The VD decreases with the increment in span-depth ratio for prestress load. Under DL, skew angle and span-depth ratio have a greater impact. Thus, the skewed bridge may be preferred over the straight bridge.
- Evident that the significant parameters affecting bending and deflection behaviour are span-depth ratio and skew angle. The span-depth ratio changes after 16 do not appreciably influence overall structural behaviour. The combined effect of span and skewness are the significant parameter that influence the shear behaviour.
- Evidence shows that the dominance of prestress load may be reduced with the skewness.

Acknowledgements
Not applicable.

Authors' contributions
Author 1: Preeti Agarwal. Literature review, Modelling and analysis, etc. Author 2: Deepak Kumar Singh. Supervision, Compiling of the paper, etc.

Funding
No sources of funding for the research reported.

Availability of data and materials
Some or all data, models, or code that support the findings of this study are available from the corresponding author upon reasonable request.
1. A bridge is modelled in CSiBridge software that can be provided,
2. Datasheet which was prepared in Excel along with graphs prepared in the Origin graph can also be provided.

Declarations

Competing interests
There is no conflict of interest.

Received: 15 May 2023 Accepted: 7 June 2023
Published online: 01 July 2023

References

Agarwal P, Pal P, Mehta PK (2019) Analysis of RC skew box girder bridges. Int J Sci Innov Eng Technol 6:1–8. (ISBN: 978-93-81288-18-4). https://www.ijsiet.org/vol62019/1.pdf
Agarwal P, Pal P, Mehta PK (2020a) Finite element analysis of skew box-girder bridges under IRC-A loading. J Struct Eng 47(3):243–258. https://serc.res.in/jose-contents
Agarwal P, Pal P, Mehta PK (2020b) Parametric study on skew-curved RC box girder bridges. Structures 28:380–388. https://doi.org/10.1016/j.istruc.2020.08.025
Agarwal P, Pal P, Mehta PK (2021) Computation of design forces and deflection in reinforced concrete skew-curved box-girder bridges. Struct Eng Mech 78(3):255–267. https://doi.org/10.12989/sem.2021.78.3.255
Agarwal P, Pal P, Mehta PK (2022a) Box-girder bridges - modelling and analysis. Int J Eng Model 35(1):19–42. https://doi.org/10.31534/engmod.2022.1.ri.02m
Agarwal P, Pal P, Mehta PK (2022b) Free vibration analysis of RC box-girder bridges using FEM. Sound Vib 56(2):105–125. https://doi.org/10.32604/sv.2022.014874
Bakht B (1988) Analysis of some skew bridges as right bridges. J Struct Eng 114(10):2307–2322
Barr PJ, Eberhard MO, Stanton JF (2001) Live-load distribution factors in prestressed concrete girder bridges. J Bridg Eng 6(5):298–306
Bishara AG, Liu MC, Ali ED (1993) Wheel load distribution on simply supported skew I-beam composite bridges. J Struct Eng 119(2):399–419
Brown TG, Ghali A (1975) Semi-analytic solution of skew box girder bridges. Proc Inst Civil Eng Part 2 59:487–500
Chang BST (1992) Prestress influence on shear-lag effect in continuous box-girder bridge. J Struct Eng 118:3113–3121
Conner S, Huo XS (2006) Influence of parapets and aspect ratio on live-load distribution. J Bridg Eng 11:188–196

Ebeido T, Kennedy JB (1995) Shear distribution in simply supported skew composite bridges. Can J Civ Eng 22:1143–1154
Ebeido T, Kennedy JB (1996) Shear and reaction distributions in continuous skew composite bridges. J Bridg Eng 1(4):155–165
Gupta T, Kumar M (2017) Structural response of concrete skew box-girder bridges a state-of-the-art review. Int J Bridge Eng 5(1):37–59
Gupta T, Kumar M (2018) Flexural response of skew-curved concrete box-girder bridges. Eng Struct 163:358–372
He XH, Sheng XW, Scanlon A, Linzell DG, Yu XD (2012) Skewed concrete box girder bridge static and dynamic testing and analysis. Eng Struct 39:38–49
Helba A, Kennedy JB (1995) Skew composite bridges - analyses for ultimate load. Can J Civ Eng 22:1092–1103
Hodson DJ, Barr PJ, Halling MW (2012) Live-load analysis of posttensioned box-girder bridges. J Bridge Eng 17(4):644-651
Huang Z, Liu XL (2006) Modified skew bending model for segmental bridge with unbonded tendons. J Bridg Eng 11(1):59–63
Huang H, Shenton HW, Chajes MJ (2004) Load distribution for a highly skewed bridge: testing and analysis. J Bridg Eng 9(6):558–562
Huang M, Liu JK, Law SS, Lu ZR (2011) Vibration analysis of prestressed concrete bridge subjected to moving vehicles. Interact Multiscale Mech 4(4):273–289. https://doi.org/10.12989/imm.2011.4.4.273
Hughs E, Idriss R (2006) Live-load distribution factors for prestressed concrete, spread box-girder bridge. J Bridg Eng 11(5):573–581
Huo XS, Zhang Q (2006) The effect of skewness on live load reactions at piers of continuous bridges. Struct Congr 1–8
Huo XS, Zhang Q (2008) Effect of skewness on the distribution of live load reaction at piers of skewed continuous bridges. J Bridg Eng 13(1):110–114
Khaloo AR, Mirzabozorg H (2003) Load distribution factors in simply supported skew bridges. J Bridg Eng 8(4):241–244
Menassa C, Mabsout M, Tarhini K, Frederick G (2007) Influence of skew angle on reinforced concrete slab bridges. J Bridg Eng 12(2):205–214
Mo YL, Jeng C-H, Krawinkler H (2003) Experimental and analytical studies of innovative prestressed concrete box-girder bridges. Mater Struct 36:99–107
Mohseni I, Rashid AK (2013) Transverse load distribution of skew cast-in-place concrete multicell box-girder bridges subjected to traffic condition. Lat Am J Solids Struct 10:247–262
Naser AF, Zonglin W (2013) Evaluating the performance of skewed prestressed concrete bridge after strengthening. Cent Eur J Eng 3(2):329–347
Park Ho, Jeong S, Lee S-C, Cho J-Y (2016) Flexural behavior of post-tensioned prestressed concrete girders with high-strength strands. Eng Struct 112:90–99
Xue X, Wu J, Zhou J, Li H (2018) A finite segment method for skewed box girder analysis. Math Probl Eng 2018:1–3. https://doi.org/10.1155/2018/2592613
Zhu M, Yan Z, Chen L, Lu Z, Chen YF (2019) Experimental study on composite mechanical properties of a double-deck prestressed concrete box girder. Adv Struct Eng 1–12. https://doi.org/10.1177/1369433219845150

Publisher's Note